# Ozone diurnal variations in the stratosphere and lower mesosphere, based on measurements from SABER on TIMED

Frank T. Huang,[1] Hans G. Mayr,[2] James M. Russell III,[3] and Martin G. Mlynczak[4]

Received 12 May 2010; revised 20 September 2010; accepted 29 September 2010; published 21 December 2010.

[1] We report on derived results of global zonal mean ozone diurnal variations over 24 h of local solar time, based on satellite measurements from SABER on the Thermosphere Ionosphere Mesosphere Energetics and Dynamics (TIMED) satellite, with focus on the stratosphere and lower mesosphere. On a global scale, results in this altitude range are new. We had previously reported on ozone diurnal variations, but the focus was at higher altitudes, where the variations can be relatively large. In the stratosphere, there can be systematic diurnal variations on the order of a few percent, with multiple local maxima over a day, and these can exist down to altitudes of ~31 hPa (~24 km) and lower. At these altitudes, photochemistry is expected to be less effective, and dynamics (e.g., tides) can be more important. The diurnal variations also depend on latitude and season. As a function of altitude, for low latitudes at least, the ozone diurnal variations show a pattern of local-time phase progression such that beginning at ~31 hPa the mixing ratios are smaller in the afternoon (compared to values at midnight), then (as the altitude increases) become mostly larger in the afternoon beginning from ~10 to 4.6 hPa, revert back to intermediate afternoon values near 2.2, 1.5 hPa, and again return to lower daytime values at about 1 hPa, with this last trend continuing to higher altitudes in the mesosphere. This pattern of variation is generally supported by previous results by us and by others, based on data from MLS UARS, MLS Aura, rocket-borne, and ground-based measurements.

**Citation:** Huang, F. T., H. G. Mayr, J. M. Russell III, and M. G. Mlynczak (2010), Ozone diurnal variations in the stratosphere and lower mesosphere, based on measurements from SABER on TIMED, *J. Geophys. Res.*, *115*, D24308, doi:10.1029/2010JD014484.

## 1. Introduction

[2] Understanding the global variations of atmospheric ozone is important for both scientific and practical reasons. In the following, we present derived results of ozone diurnal variations over the 24 h of local solar time (LST), with focus on the stratosphere and lower mesosphere (~31 hPa to 0.46 hPa, or ~24 to 55 km), at low and middle latitudes, and from 2004 through 2007. In this altitude range, the variations can be relatively small compared to those at higher altitudes, and generally have not been heretofore available on a global scale. Previously, results derived from ground-based instruments by others and derived by us using satellite data were provided at limited fixed locations. Our results are based on measurements from the Broadband Emission Radiometry (SABER) instrument [*Russell et al.*, 1999] on the Thermosphere-Ionosphere-Mesosphere-Energetics and Dynamics (TIMED) satellite. Comparisons are made with results based on data from the Microwave Limb Sounder (MLS) instrument [*Barath et al.*, 1993] on the Upper Atmosphere Research Satellite (UARS) [*Reber*, 1993], from the MLS [*Waters et al.*, 2006; *Froidevaux et al.*, 2008] on the Aura satellite [*Schoeberl et al.*, 2006], and from ground-based radiometers and rocket-borne photometers.

[3] Diurnal ozone variations can provide important information on the photochemistry, dynamics, and energetics of the atmosphere. In recent decades, global satellite measurements have added essential information for the understanding of ozone. Although the majority of these measurements have concentrated on the stratosphere, there have been relatively little quantitative analyses of ozone behavior over 24 h of local time in this region, in part because the variations are relatively small and in part because few instruments provided global measurements over the range of local solar times, to enable quantitative analyses. These variations not only are interesting and important by themselves, but they also can be of value when used in conjunction with other measurements that have records spanning decades, but which do not provide adequate information to estimate diurnal variations. Examples include ozone measurements from the solar backscatter ultraviolet (SBUV/2) instruments that have been flown on the series of NOAA polar orbiters over decades, and the long-term records are especially valuable. However, the SBUV/2 nominally measures data at two fixed local

[1]GEST, University of Maryland Baltimore County, Baltimore, Maryland, USA.
[2]NASA Goddard Space Flight Center, Greenbelt, Maryland, USA.
[3]Center for Atmospheric Sciences, Hampton University, Hampton, Virginia, USA.
[4]NASA Langley Research Center, Hampton, Virginia, USA.


0148-0227/10/2010JD014484

times, and the orbits of some satellites have drifted, so that the local times at which the measurements are made are also slowly changing, making calibration, continuity, and interpretation among the data sets problematical. Understanding the ozone diurnal variations over 24 h in local time would potentially help to resolve these issues.

[4] In the following, we first describe related measurements. In section 2 we discuss the SABER and MLS UARS data characteristics and the analysis used. In section 3 we present our results and comparisons with corresponding results based on MLS UARS, MLS Aura, ground-based, and rocket-borne measurements. We find that there is at least general qualitative agreement among the results based on the different measurements, even when the variations are as small as a few percent.

### 1.1. SABER and MLS UARS Measurements

[5] Unlike data from other satellites, SABER and MLS UARS measurements are sampled over the range of local times. Although the measurements are still asynoptic, they provide the potential to quantitatively estimate diurnal variations of ozone. SABER data are special in the breadth of their information content. They span the globe from the stratosphere into the lower thermosphere and provide information over the 24 h of local solar time, since the beginning of 2002. MLS UARS provides corroborative measurements from a decade earlier.

[6] This study parallels those of *Huang et al.* [2008a, 2008b], also based on SABER data. But there the focus was on higher altitudes in the upper mesosphere and the lower thermosphere, where the diurnal variations can be relatively large and can dominate. Here, the focus is in the stratosphere, where we find that the diurnal variations are relatively small (the order of a few percent) but are systematic, occurring at altitudes down to ~31 hPa (~24 km) and lower, where the effects of photochemistry are expected to be small.

[7] To provide a perspective and context, Figure 1 shows results corresponding to that of *Huang et al.* [2008a, 2008b], but based on a later data version of SABER, from 2004 through 2007. Figure 1a shows derived ozone zonal mean mixing ratios (parts per million by volume, ppmv) on pressure-latitude coordinates (100 to 0.001 hPa, within 48° of the equator) for day 85. We note that results near 100 hPa are not reliable. What makes Figure 1a different from previous plots of this type, aside from the large altitude range, is that it shows our derived zonal mean values that are averages over both local time and longitude in a consistent manner. Previous results based on other satellite data usually correspond to one local time. Figure 1b shows the percent deviation from the mean (in Figure 1a) of our estimates at 1400 local time. In our altitude of interest (~32 hPa (~24 km) up to 0.46 hPa (~55 km)), the relative variations are on the order of a few percent. We will see below that there are distinct patterns in the diurnal variations as a function of altitude in this range. Although relatively small, the diurnal variations in ozone are important in understanding the chemistry and dynamics of this region, where the ozone mixing ratios themselves are near maximum. These diurnal variations are the focus of our analysis.

[8] As discussed by *Huang et al.* [2008b, 2008a], at higher altitudes, the daytime mixing ozone ratios as represented by the values at 1400 local time are generally smaller compared to the mean (and to the nighttime values), and the percent differences can approach 80 percent or more. As can be seen in Figure 1, an exception is at altitudes near 0.01 hPa (~80 km), where the daytime values can be larger than the mean (and nighttime values).

### 1.2. Other Measurements

[9] As noted earlier, unlike TIMED and UARS, the orbital characteristics of other satellites, and/or the length of their missions (e.g., space shuttle missions), are such that the range of local solar times at which the data are taken is limited. Most satellite orbits are near Sun-synchronous, so that data are measured at one or two local times only, which remain fixed for the duration of the mission. In those cases, it is impractical to quantitatively analyze the measurements for their behavior as a function of local time. There are consequently relatively scant previous global results in the stratosphere with which to compare. *Wu and Jiang* [2005] have analyzed ozone data from a more recent version of MLS UARS data, but their results in the literature do not address diurnal variations with details. *Ricaud et al.* [1996] have presented diurnal variations of ozone based on MLS UARS data for some sample cases, from ~0.46 hPa to 0.046 hPa (~55 to 70 km), and although their altitude range is mostly outside that of interest to us, we will see that their results at 0.46 hPa (~55 km) are important in corroborating our results. *Huang et al.* [1997, 2008b] derived ozone diurnal variations over 24 h in local time, also based on MLS UARS and SABER data, from ~4.6 to 0.46 hPa (about 40 to 55 km), but the results were given for only one latitude and 1 day. In the following, we expand the altitude, latitude, and temporal coverage.

[10] Ground-based radiometers provide ozone measurements with the best local time resolution [e.g., *Haefele et al.*, 2008; *Connor et al.*, 1994; *Zommerfelds et al.*, 1989; *Ricaud et al.*, 1994], while rocket-borne photometers can also provide measurements at several local times over a day [*Lean*, 1982]. Although the vertical resolution of ground-based measurements can be relatively coarse, the researchers cited above have discussed and accounted for this issue in the retrieval process. We will see that these results are generally consistent with our results. Examples are limited because although there have been numerous other studies based on ground-based measurements, they have not concentrated on diurnal variations per se.

## 2. Data Characteristics and Analysis

### 2.1. SABER

#### 2.1.1. SABER Data Sampling and Analysis

[11] As noted earlier, SABER measurements provide the potential to estimate the variations of ozone as a function of local time over 24 h that data from other satellites generally do not provide. The SABER instrument [*Russell et al.*, 1999] views the Earth's limb to the side of the orbital plane (~74° inclination), and ozone emissions in the 9.6 $\mu$m band are used to retrieve the mixing ratios, corresponding to the line-of-sight tangent point. Measurements are made over the globe from about 100 hPa to altitudes higher than 0.001 hPa (~16 to 96 km), over 24 h in local solar time, since the beginning of 2002. This kind of information has not been available previously, especially from one

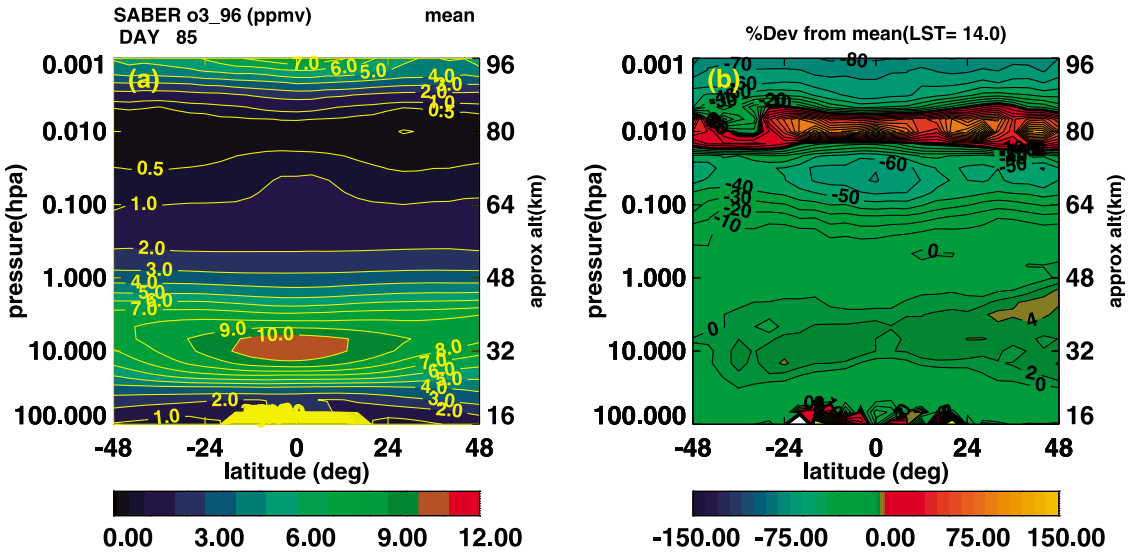


**Figure 1.** Derived zonal mean ozone mixing ratios (parts per million by volume, ppmv), based on SABER data for years 2004–2007, on altitude (100 to 0.001 hPa) versus latitude (48°S to 48°N) coordinates, for day 85 (March 26). (a) Mean values. (b) Same as Figure 1a but showing percent deviation of our estimates at 1400 LST from the mean values in Figure 1a. Values near 100 hPa are not reliable due to noisy data.

instrument. The level 2A data (version 1.07), provided by the SABER project, are interpolated to 4° latitude intervals and to pressure levels that match those of MLS on UARS and Aura, and for each day, averaged over longitude for analysis.

[12] Over a given day and for a given latitude circle, measurements are made as the satellite travels northward (ascending mode) and again as the satellite travels southward (descending mode). Data at different longitudes are sampled over 1 day as the Earth rotates relative to the orbit. The orbital characteristics of the satellite are such that over a given day, for a given latitude circle and a given orbital mode (ascending or descending), the local time at which the data are measured is essentially the same, independent of longitude and time of day. For a given day, latitude, and altitude, we work with data averaged over longitude, one for the ascending orbital mode and one for the descending mode, each corresponding to a different local solar time, resulting in two data points for each day. Each can be biased by the local time variations and is therefore not a true zonal mean. True zonal means are averages made at a specific time (not over a day) over longitude around a latitude circle, with the local solar time varying by 24 h over 360° in longitude. The local times of the SABER measurements decrease by about 12 min from day to day, and it takes 60 days to sample over the 24 h of local time. Although this provides essential information over the range of local times, over 60 days, variations can be due to both local time and other variables, such as season. Diurnal and mean variations are embedded together in the data and need to be unraveled from each other to obtain more accurate estimates of each. Therefore, although SABER (and UARS) data provide information as a function of local time that other satellites do not, the measurements are still asynoptic, and there may be inherent limitations to the information content.

[13] Our algorithm is designed for this type of sampling in local time and provides estimates of both diurnal and mean (e.g., annual, semiannual oscillations) variations together in a consistent manner. It attempts to remove the bias in the mean due to the local time. At a given latitude and altitude for data over a period of a year, the algorithm performs a least squares estimate of a two-dimensional Fourier series where the independent variables are local solar time and day of year, and variations as a function of local time and day of year over 1 year are generated. We currently do not generate results poleward of 48° latitude because data exist at the higher latitudes only on alternate yaw intervals (60 days). Because it takes SABER 60 days (36 days for MLS UARS) to sample over the range of local times, the sampling is less than ideal, and the information of the diurnal variations may be limited, and we limit the number of coefficients estimated as described in Appendix A. Once the coefficients are estimated, both the mean components and the diurnal variations can be calculated directly for any day of year. In addition to having been applied to SABER ozone measurements with focus on higher altitudes [*Huang et al.*, 2008b, 2008a] as described above, the algorithm has also been applied previously to SABER temperature measurements of diurnal variations (thermal tides) and mean variations to study intraseasonal (ISO), semiannual (SAO), and quasi-biennial (QBO) variations [*Huang et al.*, 2006a, 2006b, 2006c, 2008a]. It has also been successfully applied to wind measurements from the TIMED Doppler Interferometer (TIDI), as described by *Huang et al.* [2006a], and to MLS UARS ozone measurements [*Huang et al.*, 1997].

[14] Figure 2 shows examples of the sampling properties of SABER data and how well our algorithm estimates the data. SABER ozone mixing ratio data, averaged over longitude, at the equator and 31.6 hPa are plotted versus day for year 2005. For a given day, the solid red line and dashed green line represent the data from the ascending and descending modes, respectively, each corresponding to one local time. The two data points for each day can differ significantly from each

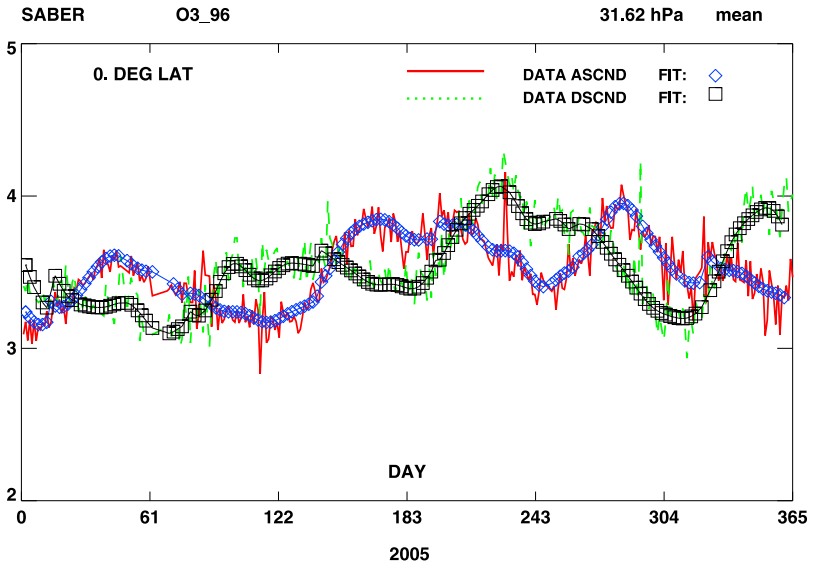


**Figure 2.** Zonally averaged SABER ozone data (ppmv) and estimated results plotted versus day of year for 2005 at the equator and 31.6 hPa. Solid red line and blue diamonds represent ascending mode data and fit, respectively. Dashed green line and black squares represent descending mode data and fit, respectively. The fits are evaluated at the same day and local time as the data (only every other point is plotted to reduce clutter).

other, reflecting different local times. The local times decrease by about 12 min from day to day. The diamonds and squares represent our fit to the ascending and descending mode data, respectively (only every other point is plotted to reduce clutter). As can be seen, the estimates approximate the measurements reasonably, although there are some intervals over several days where our estimates do not follow the data as well, so some smoothing exists.

#### 2.1.2. SABER Data Quality

[15] Previously, we had discussed the quality of the SABER data given by *Huang et al.* [2008a, 2008b], where the focus was on ozone variations at higher altitudes, from the middle mesosphere to the lower thermosphere (MLT), and where departures from local thermodynamic equilibrium (non- LTE) can be significant. This complicates the retrieval of ozone mixing ratios, and the uncertainties can be larger than those at lower altitudes. As noted by *Huang et al.* [2008a], the systematic uncertainties of the various ozone measurements in the MLT can be relatively large and can approach 50% or more at higher altitudes. Although the systematic differences become much smaller with decreasing altitude, they can still be significant.

[16] However, it is expected that the diurnal variations and mean variations (such as the quasi-biennial oscillation (QBO)), which are deviations from a more steady state, are much more robust. The following, taken from our results of ozone and temperature quasi-biennial oscillation [*Huang et al.*, 2008a] correlations, also based on SABER measurements, lends independent and additional support to the quality of the SABER data for relative variations from a mean state.

[17] Here the reason that we consider the ozone and temperature QBO is because there is more independent corroborative evidence for the ozone and temperature QBO than for the diurnal variations. In addition, there are expectations for the correlation between the ozone QBO and temperature QBO, which should provide further corroboration. As discussed earlier, diurnal and mean variations such as the QBO are embedded together in the data and need to be unraveled from each other to obtain more accurate estimates of each. From the mathematical view, the diurnal and QBO variations in the data are on equal footing, and obtaining robust estimates for the QBO reflects on that for diurnal variations, as our algorithm estimates these variations together. Figure 3 shows our derived QBO results based on SABER ozone mixing ratios (Figure 3, left, in ppmv) and temperatures (Figure 3, right, in K) at the equator on altitude versus day coordinates, based on data from 2002001 to 2004060 (the first four digits represent the year, and the last three digits stand for the day of year), assuming a period of 26 months, with the abscissa plotted over two cycles. Figures 3a and 3b show the ozone QBO (Figure 3a) and the temperature QBO (Figure 3b) between 20 and 50 km. Solid contour lines denote zero and positive values, while dashed lines denote negative values. Near 28 km (approximately the altitude of the ozone mixing ratio maximum), the QBO ozone mixing ratios undergo relatively sharp changes in phase with altitude. Below about 28 km, the ozone and temperature are just about in phase with each other as a function of day of year. Above this altitude, the ozone and temperature are mostly out of phase. The rapid change of phase in ozone near 28 km is consistent with past observations of the QBO made by *Zawodny and McCormick* [1991], *Hasebe* [1994], and *Tian et al.* [2006] using SAGE II data, and with results obtained by *Hollandsworth et al.* [1995] using SBUV data, which show a phase shift near 31 km. The stratospheric QBO has been simulated by various 1-, 2-, and 3-dimensional models, including those of *Ling and London* [1986], *Gray and Pyle* [1989], *Hasebe* [1994], *Butchart et al.* [2003], and *Tian et al.* [2006], with attendant differences in assumptions and complexities among the models. Figures 3c and 3d correspond to Figures 3a and 3b but for altitudes between 40 and 100 km. We have allowed the scales to saturate (near 40 km

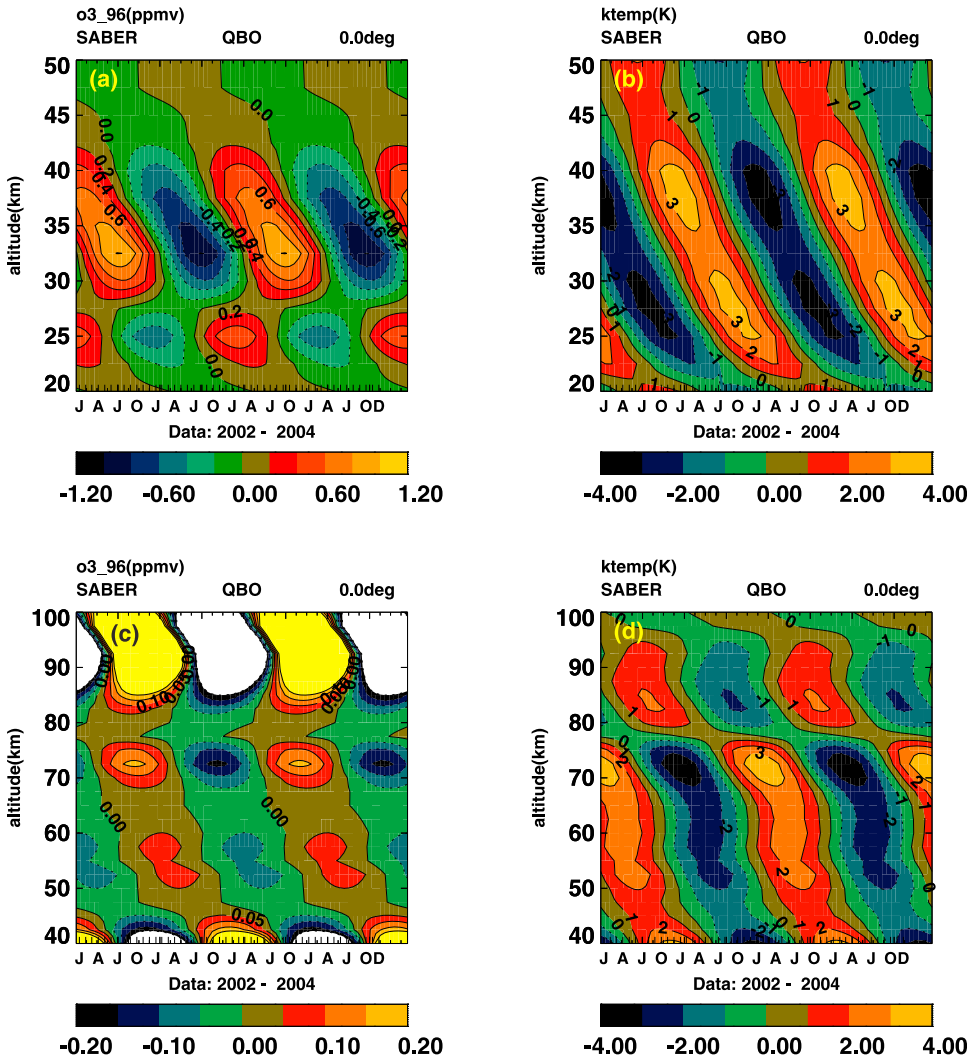


**Figure 3.** QBO results based on SABER (a) ozone (ppmv) and (b) temperatures (K) at the equator on altitude (20–50 km) day coordinates and (c and d) corresponding plots for altitudes between 40 and 100 km. The plots are over two cycles. Contour intervals are 0.2 (Figure 3a) and 0.05 ppmv for ozone, and 1 K for temperature. Solid contours denote zero and positive values; dashed lines denote negative values.

and above ~85 km) in order to show the smaller values between 45 and 85 km more clearly. It can be seen that the ozone and temperatures remain mostly out of phase with increasing altitude up to about 75 km. Between 75 and 80 km, the temperature phases change rapidly with altitude, so that above about 80 km the ozone and temperature QBOs are again more in phase with respect to day of year.

[18] The probability that the results follow the generally expected phase relationships between ozone and temperature throughout the altitude range, from the stratosphere into the mesosphere and higher, is fortuitous is extremely small. This attests to the validity of the QBO results, both for the data and the analysis. By inference, it also attests to the quality of the results of diurnal variations.

[19] We have presented a similar discussion in a related paper [*Huang et al.*, 2010] on temperature diurnal variations with focus in the stratosphere, also based on SABER measurements. For temperature diurnal variations in the stratosphere, there is additional independent corroboration of our results as reported by *Huang et al.* [2010]. In addition, separate corroboration for our estimates of the temperature QBO is discussed by *Huang et al.* [2006c]. We also note that we have presented similar discussions by *Huang et al.* [2008a, 2008b].

### 2.2. MLS UARS and MLS Aura

[20] MLS UARS, another satellite instrument that sampled over the range of local times, made measurements for some years beginning in late 1991 and obtained ozone measurements at 183 and 205 GHz. It took MLS UARS 36 days to sample over the range of local times, and discussions about issues posed by SABER data sampling also apply to MLS UARS. The results presented here are based on an early version 4 of the MLS level 3B data (205 GHz channel). The level 3B data were not archived, and the results presented here were previously generated [e.g., *Huang et al.*, 1997].

[21] MLS Aura is in a near polar, Sun-synchronous orbit and has obtained measurements from 240 GHz since 2004 [*Waters et al.*, 2006; *Froidevaux et al.*, 2008]. At low and middle latitudes, unlike the sampling of SABER and MLS UARS, the local times at which measurements are made are limited to two local times, which remain essentially the same from day to day, one for the orbital ascending mode (~1342 LST) and one for the orbital descending mode (~0142 LST). We note that the Halogen Occultation Experiment (HALOE), flown on UARS, also measured ozone in the stratosphere and mesosphere [*Brühl et al.*, 1996]. Like MLS Aura, HALOE took measurements at two local times, but at sunrise and sunset.

## 3. Results and Comparisons

[22] Our results focus on zonal mean ozone diurnal variations from ~31 hPa to 0.46 hPa (~24 to 55 km) in altitude, at low and middle latitudes, and different seasons. Comparisons are made among those based on SABER, MLS UARS, MLS Aura, rocket-borne, and ground-based measurements. We will see that the different results are at least qualitatively consistent with, and corroborate, each other. The comparisons are encouraging, especially because the variations are relatively small, mostly a few percent or less. The SABER results reflect the estimates using five Fourier harmonics in local time.

[23] Figure 4a shows derived zonal mean ozone mixing ratios versus local solar time, for day 85, at the equator, from 1 to 0.1 hPa, based on SABER measurements for year 2005. Figure 4b corresponds to Figure 4a, but for 40°N latitude. It can be seen that at higher altitudes near 0.1 hPa, the diurnal variations are more significant than that at lower altitudes. Although not shown, the diurnal variations then decrease in magnitude with altitude as the mesopause is approached. They then become much larger with altitude as indicated in Figure 1. At the higher altitudes in Figure 4, the larger variations occur near sunrise and sunset and are mostly the result of the relatively fast reactions

$$(R1) \qquad O_3 + h\nu \rightarrow O_2 + O$$

$$(R2) \qquad O + O_2 + M \rightarrow O_3 + M$$

which represent the photolysis of ozone ($O_3$) by solar radiation (R1) and the recombination of molecular ($O_2$) and atomic (O) oxygen back to ozone (R2). Molecular oxygen is relatively abundant, so the creation of ozone depends largely on the amount of available atomic oxygen. With decreasing altitude from the mesosphere on down into the stratosphere (e.g., 0.1 to 1 hPa), the diurnal variations become less significant, as daytime ozone photolysis (R1) becomes slower and conversion back to ozone (R2) becomes faster, although other reactions (e.g., $NO_x$, $ClO_x$, $HO_x$) also affect the variations of ozone over a day [see, e.g., *Vaughan*, 1984; *Allen et al.*, 1984; *Pallister and Tuck*, 1983; *Huang et al.*, 1997].

[24] As discussed below, transport by tides, at least at higher altitudes, can also affect ozone diurnal variations. In the stratosphere, our results show significant ozone diurnal variations at altitudes as low as ~31 hPa (~24 km) or lower, where photochemical effects are expected to be minimal. In a previous study [*Huang and Reber*, 2001], we found that diurnal variations are significant in the stratosphere and lower mesosphere even for $CH_4$ and $N_2O$, whose lifetimes are much longer than 1 day, suggesting that transport due to thermal tides can be important. *Haefele et al.* [2008] provide examples of diurnal variations of $H_2O$. However, this is not meant to rule out the influence of chemistry on diurnal variations at lower altitudes. As noted below, the chemical model of *Herman* [1979] generates diurnal variations near 30–35 km (~10 hPa), in agreement with our empirical results. In addition, as discussed below, the diurnal variations of ozone can also be influenced by the dependence of chemical reaction rates on temperature tides.

[25] In our altitudes of interest (below 0.46 hPa, or ~55 km), the relatively small amplitudes (approximately several percent) of diurnal variations are more difficult to discern visually in plots like Figure 4. Consequently, in the following, we consider variations with local time mostly in terms of percent deviation from their midnight value, PDVM, i.e.,

$$\mathrm{PDVM} = [(O_3(t_\ell) - O_3(t_0))/O_3(t_0)] \bullet 100,$$

where $O_3$ represents the ozone mixing ratio, $t_\ell$ the local solar time, and $t_0$ corresponds to midnight.

### 3.1. Ozone Diurnal Variations From 31.6 to 10 hPa (~24 to 31 km)

[26] We present results in this altitude range separately from that at higher altitudes, in part because the plots would otherwise be too crowded visually, and because effects from photochemistry are expected to be minimal at these lower altitudes, in which case dynamics (e.g., tides) can be more important. We do not consider altitudes below 31 hPa because the quality of the data becomes less certain. We note that due to the SABER viewing geometry, there can be data gaps of ~1 h near 1200 LST, although it does not appear there are associated problems.

#### 3.1.1. SABER Results From 31.6 to 10 hPa (~24 to 31 km)

[27] Figure 5 shows derived results in the form of percent deviation from midnight versus local time, based on SABER data at altitudes from 31.62 to 10 hPa (~24 to 31 km), year 2005, for days 85 (Figures 5a, 5c, and 5e, 26 March) and 180 (Figures 5b, 5d, and 5f, 29 June). Figures 5a and 5b correspond to 40°N latitude, while Figures 5c and 5d are for the equator, and Figures 5e and 5f are at 40°S. These plots give an indication of differences between low and middle latitudes, and solstice and equinox. Figures 5c and 5d show that at 31 hPa and the equator, the mixing ratios are mostly smaller in the afternoon (~1200 to 1800 LST) compared to morning and midnight values. With increasing altitude, at low latitudes at least, the local time phases follow a progression such that the afternoon values grow relative to midnight values, so that at 10 hPa, the afternoon values have become mostly larger than the midnight and morning values. This seems to be mostly true at midlatitudes as well, as shown in Figures 5a, 5b, 5e, and 5f, although Figure 5f, depicting results at 40°S and day 180, appears to be an exception. We will see below in Figure 7 that as a function of altitude, at least for low latitudes, the afternoon values peak near 10 and 4.6 hPa and then generally decrease relative to midnight values, such that at ~0.46 hPa the afternoon values are then generally smaller than that those at midnight. This pattern continues to higher altitudes as shown in Figure 4. As

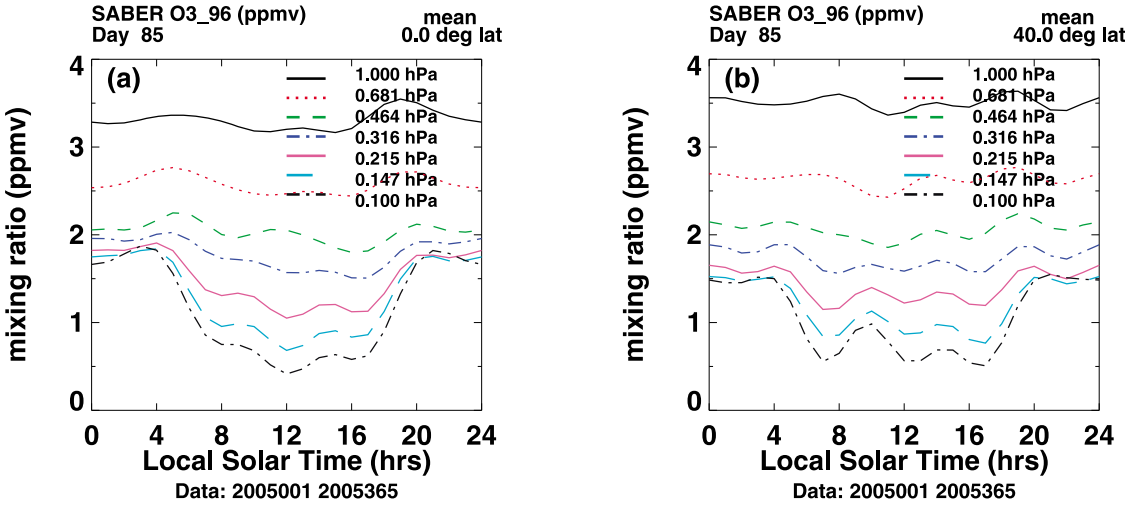


**Figure 4.** Estimated ozone mixing ratios (ppmv) versus local solar time based on SABER measurements, year 2005. (a) Day 85, 0° latitude, 1 to 0.1 hPa. (b) Same as Figure 4a but at 40°N latitude.

a function of latitude, the amplitudes of the diurnal variations are such that below ~10 hPa, the diurnal amplitudes at the equator are generally larger than those at midlatitudes (40°S and 40°N). Although the pattern (as a function of altitude) at midlatitudes is similar to those at the equator, they should be taken with more caution due to their even smaller changes in values. The SABER results are also qualitatively consistent from year to year (2004 through 2007) in this altitude range (not shown).

#### 3.1.2. Comparison With Other Results From 31.6 to 10 hPa

[28] As mentioned earlier, MLS UARS is another satellite instrument that provides sampling over the range of local times. Figure 6a shows our ozone results for day 85 at the equator, from 31.6 to 10 hPa (~24 to 31 km), based on MLS UARS measurements (205 GHz) taken over 2 plus years from 1992 to 1994. It can be seen that Figure 6a is reasonably consistent qualitatively with Figure 5c, based on SABER data at the same latitude and day of year. The MLS UARS results are smoother, and the minimum for 10 hPa in Figure 6 occurs earlier in the day, compared to Figure 5c. Quite probably, our MLS UARS results are smoother at least in part because only the diurnal and semidiurnal components were estimated for MLS UARS data, while the SABER results contain two additional local time components. Also, the data were from an early version of MLS UARS 3B data. We have not reevaluated the MLS UARS results using the same number of coefficients as for the SABER data because the MLS level 3B data were not archived and are no longer available. That MLS UARS data were made more than a decade earlier help support the reality and robustness of the results.

[29] Figure 6b shows deviations from the diurnal mean versus local time at 27.61 hPa, in Switzerland (47°N, 7°E), based on ground radiometer measurements taken from *Haefele et al.* [2008]. The results were manually transcribed from Figure 3 of *Haefele et al.* [2008] for the reader's convenience. Figure 6b can be compared to Figure 5b, at 40°, which is closer in location based on SABER data and is similar to our results at 48°N latitude for September 2005 (not shown). We have results only at 31.6 and 21.5 hPa, which straddle the 27.61 hPa in Figure 6b. Considering that the results of *Haefele et al.* [2008] are relative to the daily mean, are averaged over several weeks, and have a relatively coarse altitude resolution, while our results are relative to the midnight value and are zonal means, the agreement is qualitatively quite good, with both plots showing larger values before noon. Although our amplitude is larger, the general structures are quite similar. The most apparent difference is that shortly before midnight, there is a maximum reported by *Haefele et al.* [2008] that we do not show.

[30] Although diurnal variations of ozone due to photochemistry are not expected to be significant at these lower altitudes, the chemical model of *Herman* [1979] does show diurnal variations with amplitudes of a few percent at 30 to 35 km, consistent with our results in Figure 5 for 10 hPa (~31 km), with the afternoon values generally larger than morning values.

### 3.2. Ozone Diurnal Variations From 10 to 0.46 hPa (~31 to 55 km)

[31] Figure 7 corresponds to Figure 5, but for higher altitudes, from 10 to 0.46 hPa (~31 to 55 km), where diurnal variations are more significant, due to photochemistry. It plots the derived results based on SABER data, year 2005, in the form of percent deviation from midnight versus local time. Figures 7a and 7b show results for days 85 and 180, respectively, at 40°N latitude; Figures 7c and 7d correspond to Figures 7a and 7b, but at the equator; Figures 7e and 7f correspond to Figures 7a and 7b, but at 40°S latitude.

#### 3.2.1. Nighttime Variations

[32] As noted earlier, not all facets of ozone diurnal variations are amenable to explanation by current photochemical models alone. Examples are the post midnight changes in the ozone mixing ratios in Figures 4, 5, and 7. *Allen et al.* [1984] estimate that the nighttime density of ozone should be nearly constant from 50 km (near 1 hPa) up to about 80 km (~0.01 hPa) since the amount of existing oxygen (and hydrogen) are depleted soon after dusk. *Vaughan* [1984] states that below 65 km, atomic oxygen is almost completely converted to $O_3$ soon after dusk and the night/day

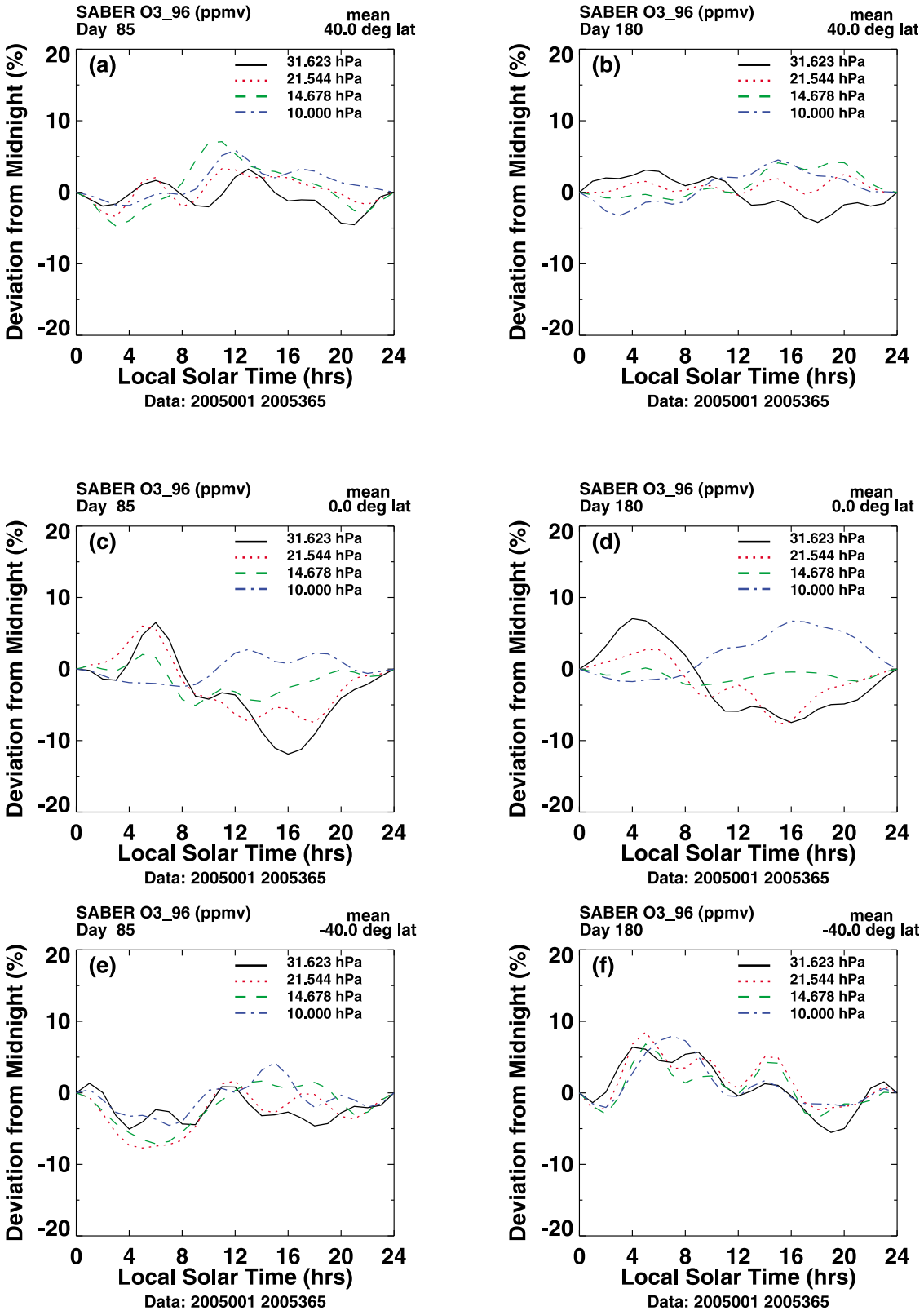


**Figure 5.** Derived results based on SABER data (year 2005), percent deviation from midnight versus local time, from 31.6 hPa to 10 hPa (~23.6 to 31 km) at 40°N latitude for days (a) 85 and (b) 180, (c and d) as in Figures 5a and 5b but for equator, and (e and f) as in Figures 5a and 5b but for 40°S latitude.

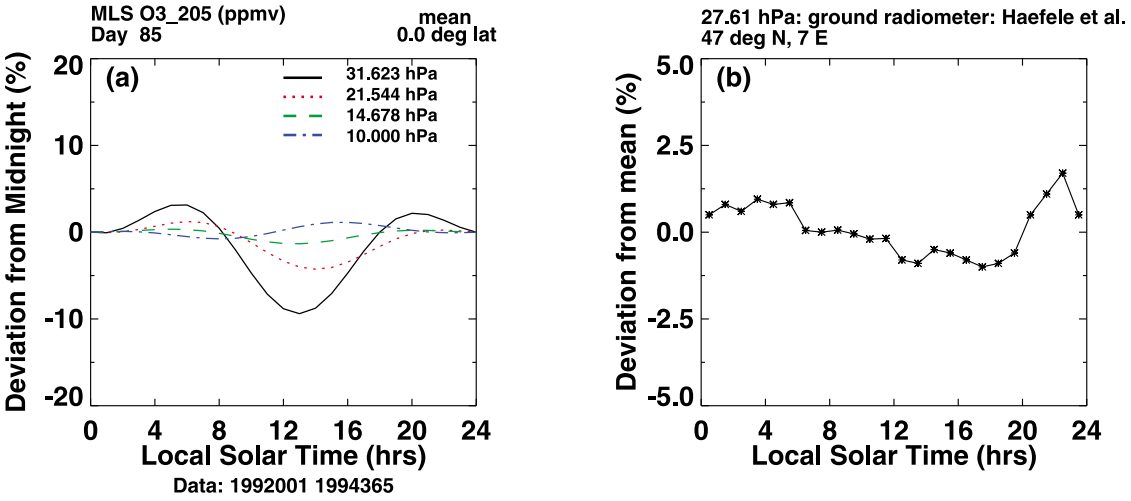


**Figure 6.** (a) Same as Figure 5 but based on MLS UARS ozone (205 GHz channel) data (years 1992–1994 merged into one 365 day period) from 31.6 hPa to 10 hPa, day 85 (26 March), at equator. Percent deviation from midnight versus local time. Note that the derived results reflect only diurnal and semidiurnal components, while results using SABER data (Figure 5) reflect twice as many Fourier coefficients in local time. (b) Ozone percent deviation from diurnal mean versus local time, based on ground radiometer data (from *Haefele et al.* [2008] for September).

ratio in ozone concentration reflects this balance. Based on ground-based microwave data, *Zommerfelds et al.* [1989] and *Connor et al.* [1994] also find postmidnight increases in the ozone mixing ratios as a function of local time in the mesosphere (although the latter state that they are intermittent and express some doubt both as to their values and their reality). *Huang et al.* [2008b] and *Huang et al.* [1997] also found postmidnight increases, based on SABER and MLS UARS data, respectively. *Zommerfelds et al.* [1989] surmise that eddy transport may explain this increase, while *Connor et al.* [1994] state that atmospheric tides are expected to cause systematic day/night variations. *Huang et al.* [1997] estimated that vertical transport due to thermal tides could account for some of the variations in the upper stratosphere and lower mesosphere but that a more complete model is needed. Other examples concerning tidal effects are also found in results at higher altitudes. *Bjarnason et al.* [1987] show that in the upper mesosphere the vertical diffusion can vary as much as 1 order of magnitude within a day as a result of large changes in the zonal wind induced by atmospheric thermal tides. In addition to the postmidnight increase, *Kaufmann et al.* [2003] suggest that the ozone equatorial maximum near 95 km (e.g., Figure 1, 0.001 hPa) is likely because of downward transport of atomic oxygen due to atmospheric tides (based on the ROSE model [*Rose and Brasseur*, 1989]), and the latitudinal distribution is also strongly biased by thermal tides.

### 3.2.2. Daytime Variations

[33] For daytime variations, a pattern that emerges from Figure 7 is that at the higher pressures near 10, 4.6, and 2.1 hPa, for low latitudes at least, the afternoon values are mostly larger than or similar to the midnight values and become mostly smaller than the midnight values with decreasing pressures near 1.0 and 0.46 hPa. This type of behavior was noted by *Huang et al.* [1997, 2008b], and expanded here to more altitudes, days, and latitudes. In section 3.2.3, we will see that this pattern is supported by measurements from both MLS UARS and MLS Aura. It is also consistent with ground-based microwave measurements [e.g., *Connor et al.*, 1994; *Haefele et al.*, 2008] and various models.

[34] Because many of the results are new and the variations in our altitudes of interest are relatively small, it is reasonable to ask about the quality and reality of the diurnal variations, in particular with respect to the existence of one or more local maxima (minima) as a function of local time, seen in Figures 7 and 5. Examples are at 0.46 hPa in Figures 7a and 7b, with distinct local maxima (sometimes secondary) near 1400 local time at 40°N, and at 35°N latitude in Figure 8a. As discussed in more detail in section 3.2.3, the results of *Lean* [1982], based on rocket-borne photometer data, of *Haefele et al.* [2008], based on ground-based radiometers, and of *Ricaud et al.* [1996], based on MLS UARS data, all corroborate the existence of these local maxima. They are also consistent with the results of *Marsh et al.* [2002], based on HRDI measurements on UARS, albeit at higher altitudes. Also providing support for our results is an explicit photochemical model [*Austin*, 1991] of the United Kingdom Meteorological Office (UKMO), which predicted the local maximum at 0.46 hPa in the early afternoon at 28°N latitude (see *Huang et al.* [1997] and discussion of Figure 8). We discuss these in more detail in the rest of the paper.

[35] Taken together, Figures 4, 5, 6, 7, and 8 show a general pattern in how the ozone diurnal variations behave as a function of altitude. For low latitudes at least, starting from 31.6 hPa (~24 km), the mixing ratios in the afternoon are mostly smaller compared to their values at midnight. As the altitude increases, the afternoon values increase relative to their midnight values, such that near 10 hPa to 2.1 hPa the afternoon values are then mostly larger than or similar to the midnight values. With the altitude continuing to increase to 1.0 and 0.46 hPa, the daytime values again become mostly smaller than the midnight values, and this last trend

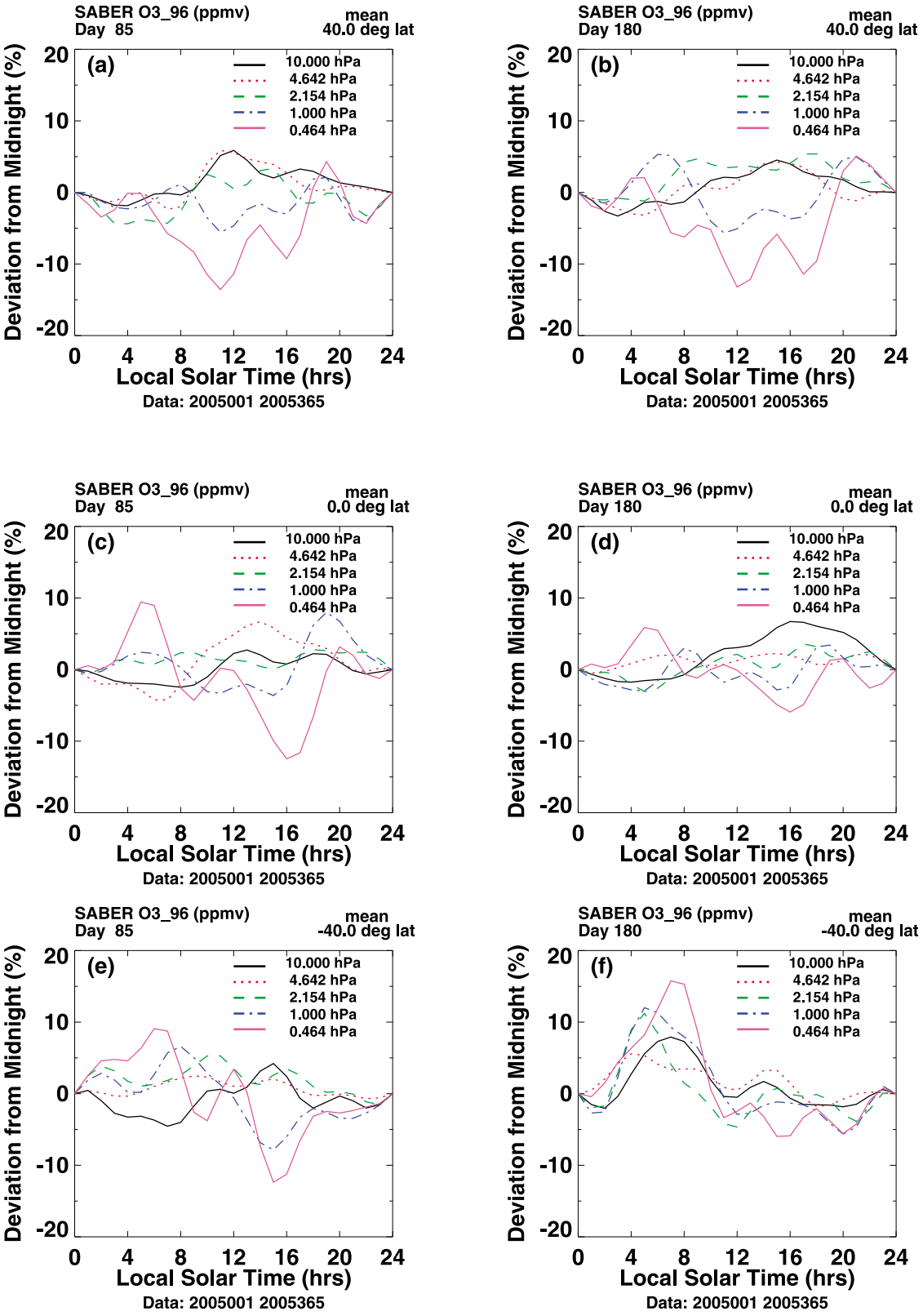


**Figure 7.** Derived results based on SABER data (year 2005), percent deviation from midnight versus local time. At 40°N latitude for days (a) 85 and (b) 180 from 10 to 0.46 hPa (~31 to 55 km), (c and d) same as Figures 7a and 7b but for equator, and (e and f) same as Figures 7a and 7b but for 40°S.

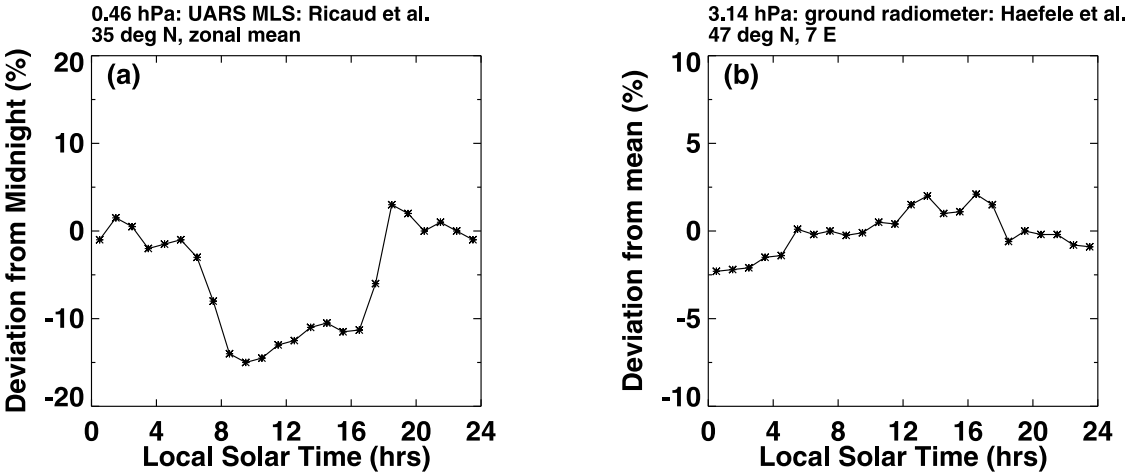


**Figure 8.** (a) Ozone percent deviation from night value versus local time, based on MLS UARS data for October, transcribed from *Ricaud et al.* [1996]. (b) Percent deviation from diurnal mean based on microwave radiometer data for September/October, transcribed from *Haefele et al.* [2008].

continues into the middle and upper mesosphere. This pattern at lower altitudes (beginning at ~24 km, 31 hPa) has not been realized previously, and at higher altitudes, our results expand upon that noted earlier [*Huang et al.*, 2008b, 1997].

[36] Although not shown, the SABER results are also qualitatively consistent from year to year.

### 3.2.3. Comparison With Other Results From 10 to 0.46 hPa (~31 to 55 km)

[37] In this section, we compare our results with corresponding results by others, based on various measurements. Although results in Figure 7 do not always correspond to the same location and time as the other results, where feasible, we have evaluated our results near those locations. Unless otherwise noted, these results are consistent with those discussed in Figure 7.

[38] Earlier, we mentioned the existence of local maxima in local time shortly after noon seen in Figures 7a and 7b at 0.46 hPa (~55 km), 40°N latitude. *Ricaud et al.* [1996] have presented diurnal variations of ozone based on MLS UARS (183 GHz instrument) for sample cases. Because the asynoptic sampling of MLS UARS data are similar to those of SABER, they note, as we have, that if there are trends in the 36 days it takes to sample the data over the range of local times, then changes in ozone may well be induced more by monthly variations than by diurnal effects in the sampled data. Unlike the analysis we use, *Ricaud et al.* [1996] do not attempt to account for contamination of the diurnal variations from seasonal variations. Consequently, they restricted their analysis to altitudes where the diurnal variations are larger than 10% of the diurnal average, and the lowest altitude for which they have results is 0.46 hPa (~55 km). For convenience, we have manually transcribed their Figure 5a (35°N latitude, October 1991 and 1992, zonal mean, ratio to nighttime value) and also transformed the values to percent deviations from night, as shown in Figure 8a. They state that their result "shows a daytime maximum at 1400 LST. This maximum is consistent with the faster photodissociation of $O_2$ at the lower latitude leading to a higher rate of ozone formation from the three-body reaction of O with $O_2$ before $HO_x$ catalytic cycles cause $O_3$ to decrease." This can be compared with Figures 7a and 7b. We both also show peaks near 0600 and 1800 LST, and local maxima near 1400 LST. Our local maximum near 1400 LST is more prominent than that of *Ricaud et al.* [1996], which can be due in part to the fact that each point in the results of *Ricaud et al.* [1996], as shown in Figure 8a, is from a different day over 36 days and thereby also reflects seasonal variations in the data. On the other hand, our results correspond to 1 day, since we have attempted to account for seasonal variations.

[39] As with results in Figure 5, where we had noted earlier that the ground-based results of *Haefele et al.* [2008] agreed well with our results near 27.61 hPa, Figures 7a and 7b (40°N latitude) can also be compared to the ground-based results of *Haefele et al.* [2008], who show results at 0.55 and 3.14 hPa. We have also manually transcribed the results of *Haefele et al.* [2008] at 3.14 hPa and 47°N latitude to Figure 8b. Their pressure surface is not the same as ours, and their values are relative to the daily mean rather than to midnight. Our results in Figures 7a and 7b at 40°N and 2.1 and 4.6 hPa straddle their 3.14 hPa results, and it can be seen that our results are similar to those of *Haefele et al.* [2008]. For their results at 0.55 hPa (not shown), our results in Figures 7a and 7b at 1.0 and 0.46 hPa straddle 0.55 hPa, and we both show local peaks near 0600 and 2000 LST, also consistent with the work by *Ricaud et al.* [1996], noted earlier. Also in agreement with our results and those of *Ricaud et al.* [1996], they show a local maximum with respect to local time that starts near noon and peaks near 1500 LST, although the amplitude appears to be smaller than ours. *Connor et al.* [1994] also provide results derived from ground-based spectrometers at Table Mountain, California (34.4°N, 117.7°W, June 1991, October 1990), at 0.75 hPa and 3.2 hPa. They present results in absolute values (ppmv), so comparisons are not as readily made. However, consistent with our results and those of others, at 0.75 hPa (their Figure 5a), they show maxima near 0600 and 1800 LST, and also near 1400 LST. At 3.2 hPa, their relative variations are similar to ours as well. The smoother variations in the ground-based results may in part be due to that they are averaged over weeks or more. *Marsh et al.* [2002], in discussing their results based on HRDI on

UARS (at higher altitudes), state "Variations in local time are much larger than the variations seen by ground based techniques, but this is likely due to the fact that the vertical resolution of the microwave technique would tend to smear out much of the fine vertical structure." However, we should note that although the daytime variations of the results by *Haefele et al.* [2008] at 0.55 hPa appear to be smoother than our results, their maximum difference between day-night values are larger than ours. In section 2.1.1 we discussed caveats of analyzing SABER data.

[40] *Lean* [1982] has presented results of rocket-borne photometer measurements at Wallops Island (~37.84°N, 75.48°W), from 35 to 60 km (~5.7 to 0.2 hPa), October 1979, at four different local times (~0900–1000 LST, ~1200–1400 LST, sunset, and night). Her Figure 6 can also be compared to our Figures 7a and 7b, for 10 to 0.46 hPa (~31 to 55 km, 40°N latitude). At 55 km (~0.46 hPa), *Lean* [1982] shows a local maximum from ~1200 to 1400 LST (relative to ~0900 to 1000 LST), consistent with our Figures 7a and 7b. At 35 and 40 km, *Lean* [1982] and we (see 10 and 4.6 hPa in our Figures 7a and 7b) both show that the values at 1200–1400 LST are larger than the values near 0900 to 1000 LST. At 50 km, *Lean* [1982] and we (see 1.0 hPa in our Figures 7a and 7b) both show that the early afternoon values are smaller than those near 0900 to 1000 LST. Qualitatively, the comparisons are therefore very good. More detailed comparisons are difficult, because the local time resolution of *Lean* [1982] is not good, as the values between 1200 and 1400 LST and between 0900 and 1000 LST are flat. In any event, the results of *Lean* [1982], in agreement with the results by *Ricaud et al.* [1996] and the ground-based results, provide clear support for the existence of the daytime local maxima just after noon.

[41] Furthermore, as can be seen in Figure 4, the daytime variations reflect a smooth transition as the altitude increases from 1 to 0.1 hPa. At higher altitudes (~70 to 82.5 km or ~0.052 to 0.0069 hPa), *Marsh et al.* [2002] also find instances of one or more local maxima over the 12 h of daytime ozone variations derived from the High Resolution Doppler Imager (HRDI) measurements on UARS. At the equator, they show a minimum near 1200 LST and distinct maximum near 1300 LST at 70 km (~0.052 hPa) and at 72.5 km. *Huang et al.* [2008b] compared their results with those by *Marsh et al.* [2002], and the relative variations are good, although our mean values are generally somewhat larger.

[42] MLS Aura makes measurements at only two fixed local times for all days, namely, at ~1342 and ~0142 LST. We have compared zonal mean MLS Aura at 0142 and 1342 LST at the equator, as a function of day of year for 2005 with our results based on SABER data shown in Figure 7 at the equator (see Figure 7c). We both show the following: (1) at 10 hPa the afternoon (1342 LST) and night (0142 LST) values are about the same over the year, (2) at 4.64 hPa the daytime values are larger than the nighttime values by a few percent, and at 2.15 hPa the daytime and nighttime values are again comparable, and (3) at 1.0 hPa the daytime values become slightly smaller relative to the nighttime values, and at 0.46 hPa (~55 km) and 0.1 hPa (~64 km) the daytime values become progressively smaller (approximately a few percent, ~50 percent) compared to the nighttime values. It is unlikely that this consistency over these six pressure surfaces is fortuitous. The comparisons for day 180 (Figure 7d) are also good, although at 4.6 hPa our afternoon values are closer to the midnight values than the corresponding values on day 85. The consistency of MLS Aura data with SABER results is significant especially because we are dealing with relatively small variations. At the still lower altitudes below 10 hPa, data from MLS Aura mostly, but not always, support the results based on SABER data. We note that the systematic differences between SABER and MLS Aura results can be significantly larger, and can approach 10 percent or more in some cases. However, these are not unexpected, as systematic uncertainties among various measurements have been reported previously [e.g., *Froidevaux et al.*, 2008; *Huang et al.*, 2008a, 2008b]. The systematic differences appear to be more in the form of offsets, and the SABER and MLS Aura data seem to correlate well as a function of day of year. Our results of diurnal variations are based on relative variations, and are much more robust.

[43] Figure 9 corresponds to results given by *Huang et al.* [2008b], updated to reflect the current version of SABER data, and plotted in pressure versus local time coordinates. The plots show derived results of zonal mean ozone percentage deviations from midnight values versus local solar time, at 28°N from 4.6 to 0.46 hPa (~36 to 55 km), chosen to compare with results from the United Kingdom Meteorological Office (UKMO) chemical model [*Huang et al.*, 1997]. The SABER results are based on data from 2004–2007 (Figure 9a), and the MLS UARS data are from 1992 to 1994. It is important to first note that the derived results based on MLS data reflects only diurnal and semidiurnal components (explained later), while Figure 9a, using SABER data, reflects twice as many Fourier coefficients in local time. As with Figure 7, of significance is that results derived from SABER and MLS both show a change in regime from larger daytime (compared to midnight) values beginning from 4.6 hPa, to intermediate daytime values near 3.2, 2.2, 1.5 hPa, to lower daytime values at about 1 to 0.46 hPa. The intermediate values based on SABER and MLS data compare to better than a few percent, and as shown by *Huang et al.* [1997], the UKMO chemical model also agreed quite well with these results. The UKMO model also showed the local maximum in midafternoon at 0.68 and 0.46 hPa as in Figure 9a, but not found in Figure 9b at 0.46 hPa, based on MLS data. This is probably because the derived results based on MLS data reflects only diurnal and semidiurnal Fourier components, while Figure 9a, using SABER data, reflects twice as many Fourier coefficients in local time. Also, recall the discussion concerning Figure 8a (second paragraph of this section), where *Ricaud et al.* [1996], also using MLS data (but from the 183 GHz data versus the 205 GHz data used by us), also show the existence of the local afternoon maximum. When the UKMO results were restricted to two Fourier components, the local maximum at midafternoon also disappeared. This lends confidence to both the data results and the model. We have not reevaluated the MLS UARS results using the same number of coefficients as for the SABER data because the MLS level 3B data were not archived and are no longer available. Also, the MLS level 3B data used for Figure 9 are from a very early data version. The similarity between the left and right plots of Figure 9 show that although interan-

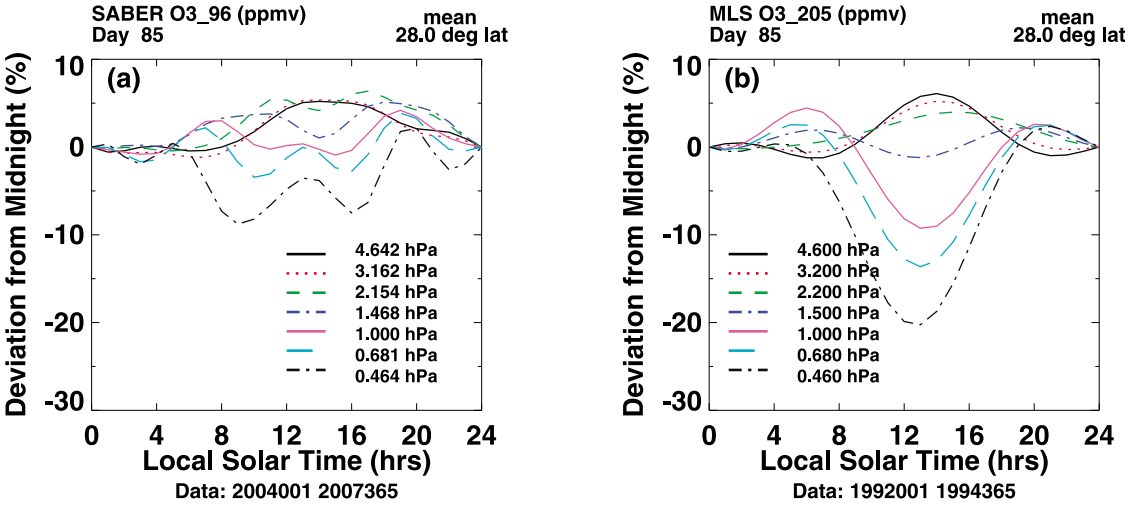


**Figure 9.** (a) Percent deviation from midnight value of ozone mixing ratios (ppmv) for day 85, 28°N, as a function of local solar time from 4.6 to 0.46 hPa (~36 to 55 km) based on SABER data from 2004 to 2007 merged together. (b) Same as Figure 9a but based on MLS UARS data (years 1992–1994). Figure 9b reflects only diurnal and semidiurnal components, while Figure 9a reflects twice as many local time components.

nual variations exist, the basic patterns hold. Although there are now new versions of the MLS UARS data, and the UKMO model results are more than 10 years old, the likelihood of a fortuitous agreement between the two data sets and with the model is small.

[44] Figures 6a and 9c together shows the local time phase progression from 31.6 to 0.46 hPa based on MLS UARS measurements, in agreement with Figures 5 and 7, based on SABER data.

### 3.3. Model Comparisons and Considerations

[45] Our results can be useful in interpreting and verifying model calculations. Earlier, we had noted that the post-midnight increase in ozone mixing ratios is not readily amenable to explanation by photochemical models alone, and that in the mesosphere, *Zommerfelds et al.* [1989] and *Kaufmann et al.* [2003] suggested that transport by tides is a major consideration. Also, *Marsh et al.* [2002] noted clear dynamical signatures in the distributions of ozone in the mesosphere, based on HRDI data, stating that they are indications of vertical advection of atomic oxygen by the solar diurnal tide, which plays an important role in determining ozone concentrations. In our lower altitudes of interest, the diurnal thermal tide amplitudes are smaller, with temperature amplitudes up to ~5 K at 0.46 hPa (~55 km), and decreasing to ~1 K or less near 4.6 hPa (~40 km) and lower, as described in a corresponding study on tidal temperatures [*Huang et al.*, 2010]. The existence in our results of diurnal variations of ozone at lower altitudes (e.g., below 10 hPa) points to the need to consider dynamics, where photochemical effects are not expected to be significant.

[46] In the stratosphere, there have been relatively fewer studies on the tradeoffs between dynamics and photochemistry over a diurnal cycle. For longer time scales, these tradeoffs in studying ozone concentration have been studied in more detail. It is thought that above ~10 hPa, ozone is controlled more by chemistry, while dynamics have more influence at lower altitudes.

[47] Among others, *Finger et al.* [1995] analyzed ozone data from the Solar Backscatter Ultraviolet Radiometer (SBUV) and the temperature analysis from the National Centers for Environmental Prediction, Climate Prediction Center (NCEP/CPC), taken over more than a decade. Generally, they found an overall positive correlation between ozone and temperature in the lower stratosphere and a mostly negative correlation in the upper stratosphere. See also the discussion related to Figure 3, and see *Huang et al.* [2008a]. However, *Rood and Douglass* [1985] and *Douglass et al.* [1985] show that dynamics can also cause significant anticorrelations between temperature and ozone, so the situation may not always be simple to interpret. Based on chemistry alone, the dependence on temperature of ozone chemical reaction rates leads to negative correlations between ozone and temperature perturbations, as was demonstrated by *Barnett et al.* [1975]. Temperature tidal variations can also be important in determining ozone concentrations. For time scales of 1 day or less, which are more pertinent to this study, there have been few analyses. For these smaller periods, the response times of ozone and temperature to each other, in order to maintain equilibrium, has been studied by *Froidevaux et al.* [1989]. They use a daytime chemical model at midlatitudes, with input temperature perturbations of various periods less than 1 day, and compare the ozone response in the form of the magnitude of the correlation coefficient, [r]. At 5 hPa, the effective ozone response is not significant ([r] ~0.1) but becomes more evident with increasing altitude, with [r] ~0.8 or more near 1 hPa. Therefore, over a diurnal cycle, ozone and temperature variations in the upper stratosphere are expected to be correlated to varying degrees. As noted earlier, we have derived results for diurnal temperature variations in this altitude range, based on SABER temperature measurements [*Huang et al.*, 2010]. The

diurnal amplitudes are up to ~5 K near 0.46 (~55 km) and are generally less than 1 K below ~10 hPa (~31 km), while the semidiurnal amplitudes are generally less than 1°K throughout this altitude range.

[48] Consequently, full 3-D chemistry-climate models with tidal variations are needed to realistically study details of ozone diurnal variations. In addition to empirically based results described in section 3.2.3, *Haefele et al.* [2008] have also provided ozone diurnal variations generated by two comprehensive 3-D models which can be directly compared to our and their results at 27.62, 3.14, and 0.55 hPa. The comparisons of our results with the models are very good at 3.14 hPa, not as good at 0.55 hPa, and poor at 27.61. At 0.55 hPa the models do not show the local maxima near 0600, 1400, and 1800 LST that are in our results, in the ground-based results of *Haefele et al.* [2008] and *Connor et al.* [1994], and in the results of *Ricaud et al.* [1996], as discussed earlier. At 27.61 hPa, the model amplitudes are much smaller (< ~0.2 percent versus ~1 percent) than our and Haefele's results, and the phases do not agree.

## 4. Seasonal Variations

[49] In order to more efficiently provide an indication of diurnal variations over space and time, Figure 10a plots the amplitude (ppmv) of the ozone diurnal component at the equator, on altitude versus day coordinates based on SABER data from 2004 through 2007, with the data merged into one 365 day period. Figure 10b corresponds to Figure 10a but for phases (local time hour of maximum value). Although the diurnal component alone does not represent all of the ozone variations, at higher altitudes, it can provide an indication of the order-of-magnitude variations over an annual cycle. As can be seen, there are evident semiannual variations in the diurnal amplitudes themselves. The phase plot of the diurnal component is consistent with the phase progression of the overall ozone variation as a function of altitude discussed earlier for Figures 5 and 7, showing the shift of the time of maximum values to the afternoon (compared to midnight values) from lower altitudes and back smaller afternoon values as the altitude increases above ~1 hPa. The results based on data for individual years (not shown) are qualitatively consistent, showing that the results are robust from year to year, although there are interannual variations. Note that the large amplitudes near 100 hPa are not reliable due to anomalies in the data.

## 5. Summary and Discussion

[50] We have derived results of zonal mean ozone diurnal variations over 24 h in local time, based on data from SABER and from MLS UARS, with focus on the stratosphere and lower mesosphere. The results cover low and middle latitudes, and over an annual cycle. On a global scale, these results have not been available previously. Our results show that diurnal variations in ozone can be systematic, with magnitudes of up to a few percent, at altitudes as low as 31 hPa (~24 km), and there can be multiple local maxima as a function of local time. Because of the relatively small amplitudes and because much of the results are new, we have compared our results with those by others, based on various measurements. There is at least good general qualitative agreement with them all.

[51] At the lower altitudes in our region of interest (below 10 hPa or ~31 km), our results based on SABER data agree reasonably well with our results based on MLS UARS data (see discussion relating to Figure 6a), with ground-based results given by *Haefele et al.* [2008] near 27 hPa, and with the chemical model of *Herman* [1979] near 30 km. At higher altitudes, there are also only limited results with which to compare. Near 0.46 hPa (~55 km), the results of *Ricaud et al.* [1996], based on MLS UARS, of *Haefele et al.* [2008] and *Connor et al.* [1994], based on ground-based radiometers, and our results, based on SABER data, are all consistent with each other. We all show local peaks near 0600 and 1800 LST, and local maxima near 1400 LST. Results from *Lean* [1982], based on rocket-borne photometer data, also show the local maxima in the afternoon (variations before 0600 and after 1800 LST are not provided). Near 3.1 hPa and midlatitudes, our results are also consistent with those of *Haefele et al.* [2008], *Connor et al.* [1994], and *Lean* [1982]. There is also good qualitative agreement with results from both MLS UARS (see discussion relative to Figure 8) and MLS Aura over a range of altitudes. The main exception is that MLS Aura data at ~31 hPa are inconsistent with results based on SABER and MLS UARS data. However, the ground-based results by *Haefele et al.* [2008] at ~27 hPa agree well with our results of between 31 and 21 hPa, based on SABER data. We also note that although our results near 30 km agree well with the model results of *Herman* [1979], that model, like some other models, does not show the afternoon local maxima at 0.46 hPa (~55 km). However, the UKMO chemical model does show the local maxima at 0.46 hPa. These local maxima also show a smooth transition to higher altitudes in the mesosphere, where the results also show one or more daytime local maxima [*Huang et al.*, 2008b], and are consistent with results from *Marsh et al.* [2002], based on measurements from HRDI on UARS.

[52] As a function of altitude, for low latitudes in particular, the ozone diurnal variations show a pattern of phase progression in local time, such that beginning at ~31 hPa, the mixing ratios are mostly smaller in the afternoon compared to midnight values. As the altitude increases, the afternoon values grow relative to their values at midnight, so that beginning from ~10 to 4.6 hPa, the mixing ratios in the afternoon are mostly larger than or similar to the midnight values. As the altitude continues to increase to near 1.0 hPa, the afternoon values again become smaller than the midnight values. This last trend continues with ever decreasing daytime values to higher altitudes in the mesosphere. This pattern, beginning at lower altitudes (~24 km, 31 hPa) has not been realized previously, and at higher altitudes, our results expand upon that noted earlier [*Huang et al.*, 1997; *Huang et al.*, 2008b], and by chemical models. It is also consistent with results based on SABER, MLS UARS, MLS Aura, on rocket-borne photometers, and on ground-based microwave techniques.

[53] As a function of latitude, the amplitudes of the diurnal variations are such that below ~10 hPa, the amplitudes at the equator are generally larger than those at midlatitudes. Our results also show that the ozone diurnal variations are qualitatively consistent from year to year, based on SABER data

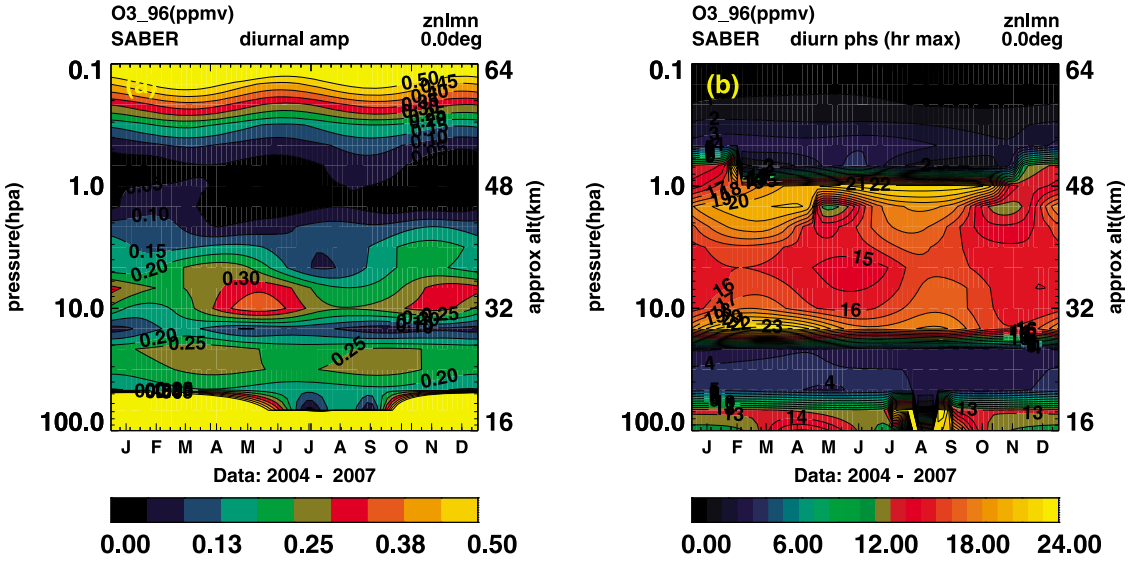


**Figure 10.** (a) Derived amplitude of ozone diurnal component on altitude (100 to 0.1 hPa) versus day coordinates at the equator, based on SABER data from 2004 through 2007 merged into one 365 day period. (b) Same as Figure 10a but for phases (local time of maximum value). Note that large amplitudes near 100 hPa are not reliable.

from 2004 through 2007, and based on MLS UARS data, which were taken more than a decade earlier.

[54] Because it is usually thought that effects of photochemistry are not significant at altitudes below ~10 hPa (~32 km), the existence of diurnal ozone variations found by *Haefele et al.* [2008] at midlatitudes near 27 hPa, and by us more globally, merits further study. In addition, our results show larger variations at the equator and ~31 hPa (~24 km) that can be ~5 percent. We and others have noted that tidal considerations are important in the mesosphere. There have been relatively fewer investigations in the stratosphere, where both tidal and photochemical effects are smaller than at higher altitudes. Also, chemical reaction rates can depend on tidal temperatures. *Huang et al.* [2010] show that diurnal tidal amplitudes in temperature is ~1 K near 30 km at low latitudes, which compares very well with those of *Zeng et al.* [2008], based on data from the Challenging Minisatellite Payload (CHAMP).

[55] Our comprehensive and detailed results are especially well suited for further comprehensive comparisons with global 3-D chemistry climate models, and we plan efforts in that direction. The results can also be important because the information can be used in conjunction with other data sets that do not provide adequate information in terms of local time but which are important because the data have a time span of decades.

## Appendix A: Data Analysis Algorithm

[56] For a given latitude and altitude, the algorithm performs a two-dimensional Fourier least squares analysis in the form

$$\Psi(t_1, d, z, \theta, \lambda) = \sum_n \sum_k b_{nk}(z, \theta, \lambda)\, e^{i2\pi n t_1} e^{i2\pi k d/N} \qquad (A1)$$

where $\Psi(t_1, d, z, \theta, \lambda)$ represents the input data; z is altitude; d is day of year; $\theta$ latitude; $\lambda$ longitude (radians); $t_1$ = local solar time (fraction of a day) = $t + \lambda/2\pi$; t = time of day (fraction of day), and N is the number of days in the fundamental period. For example, if we analyze data over 1 year, then N = 365.

[57] In this study, we apply the algorithm to data averaged over longitude, although it has been applied to data with longitude variations as well [see *Huang and Reber*, 2004]. For variations with longitude, we use data at discrete longitudes $\{\lambda_i\}$ to find the set $b_{nk}(z, \theta, \lambda_i)$ from (A1). To analyze the behavior with longitude, we estimate $\alpha_{mnk}(z, \theta)$ from

$$b_{nk}(z, \theta, \lambda_i) = \sum_m \alpha_{mnk}(z, \theta) e^{i2\pi m \lambda_i/2\pi} \qquad (A2)$$

again using a least squares fit. Finally, for any day of year $d_0$, we can sum (A1) over k to obtain

$$\Psi(t, d_0, z, \theta, \lambda) = \sum_m \sum_n \beta_{nm}(z, \theta) e^{i2\pi m \lambda/2\pi} e^{i2\pi n t} \qquad (A3)$$

where we use $\beta_{nm}$ to denote the transform to universal time t (fraction of a day).

[58] If we average the data over longitude, then we obtain the migrating diurnal variations and mean flows [*Huang and Reber*, 2003] from (A1), where the coefficients are no longer dependent on $\lambda$. Once we have estimated the coefficients in (A1) or (A3), we can directly generate the diurnal variations for composition, winds, and temperature as a function of day of year, longitude, and time. TIMED sampling patterns are such that data at latitudes poleward of about 50° are made only for alternate yaw periods. Therefore, our current analyses are made only within 48° of the equator.

[59] Our fits to the data are based on data over a period of one year or more. Currently in (A1), the maximum value of

n is 5 for ozone, and the maximum of k depends on the fundamental period in day of year. Because it takes SABER 60 days to sample over the range of local times, when the fundamental day-of-year period is 365 days, we estimate the coefficients $b_{nk}$ (z, $\theta$, $\lambda_i$) for k greater than or equal to 3 only for n = 0, and the maximum of k is 6. When the fundamental period corresponds to the QBO, the number of terms for day of year is scaled up accordingly. The current version of the data does not provide for uncertainties, and we also assume that the uncertainties of the data are proportional to the data values themselves.

[60] **Acknowledgments.** We thank Editor Joost de Gouw, and three reviewers for insightful comments that improved this paper. F.T. Huang was supported under a NASA contract to the Goddard Earth Sciences and Technology Center (GEST), University of Maryland Baltimore County.

## References

Allen, M., J. I. Lunine, and Y. L. Yung (1984), The vertical distribution of ozone in the mesosphere and lower thermosphere, *J. Geophys. Res.*, *89*(D3), 4841–4872, doi:10.1029/JD089iD03p04841.

Austin, J. (1991), On the explicit versus family solution of the fully diurnal photochemical equations of the stratosphere, *J. Geophys. Res.*, *96*(D7), 12,941–12,974, doi:10.1029/90JD02446.

Barath, F. T., et al. (1993), The Upper Atmosphere Research Satellite Microwave Limb Sounder Instrument, *J. Geophys. Res.*, *98*(D6), 10,751–10,762, doi:10.1029/93JD00798.

Barnett, J. J., J. T. Houghton, and A. J. Pyle (1975), Temperature dependence of the ozone concentration near the stratopause, *Q. J. R. Meteorol. Soc.*, *101*, 245–257, doi:10.1002/qj.49710142808.

Bjarnason, G. G., S. Solomon, and R. R. Garcia (1987), Tidal influences on vertical diffusion and diurnal variability of ozone in the thermosphere, *J. Geophys. Res.*, *92*(D5), 5609–5620, doi:10.1029/JD092iD05p05609.

Brühl, C., et al. (1996), Halogen Occultation Experiment ozone channel validation, *J. Geophys. Res.*, *101*(D6), 10,217–10,240, doi:10.1029/95JD02031.

Butchart, N., A. A. Scaife, J. Austin, S. H. E. Hare, and J. R. Knight (2003), Quasi-biennial oscillation in ozone in a coupled chemistry climate model, *J. Geophys. Res.*, *108*(D15), 4486, doi:10.1029/2002JD003004.

Connor, B. J., D. E. Siskind, J. J. Tsou, A. Parrish, and E. E. Remsberg (1994), Ground-based microwave observations of ozone in the upper stratosphere and mesosphere, *J. Geophys. Res.*, *99*(D8), 16,757–16,770, doi:10.1029/94JD01153.

Douglass, A. R., R. B. Rood, and R. S. Stolarski (1985), Interpretation of ozone temperature correlations: 2. Analysis of SBUV ozone data, *J. Geophys. Res.*, *90*(D6), 10,693–10,708, doi:10.1029/JD090iD06p10693.

Finger, F. G., R. M. Nagatani, M. E. Gelman, C. S. Long, and A. J. Miller (1995), Consistency between variations of ozone and temperature in the stratosphere, *Geophys. Res. Lett.*, *22*(24), 3477–3480, doi:10.1029/95GL02786.

Froidevaux, L., M. Allen, S. Berman, and A. Daughton (1989), The mean ozone profile and its temperature sensitivity in the upper stratosphere and lower mesosphere: An analysis of LIMS observations, *J. Geophys. Res.*, *94*(D5), 6389–6417, doi:10.1029/JD094iD05p06389.

Froidevaux, L., et al. (2008), Validation of Aura microwave limb sounder stratospheric ozone measurements, *J. Geophys. Res.*, *113*, D15S20, doi:10.1029/2007JD008771.

Gray, L. J., and J. A. Pyle (1989), A two-dimensional model of the quasi-biennial oscillation of ozone, *J. Atmos. Sci.*, *46*, 203–220, doi:10.1175/1520-0469(1989)046<0203:ATDMOT>2.0.CO;2.

Haefele, A., K. Hocke, N. Kämpfer, P. Keckhut, M. Marchand, S. Bekki, B. Morel, T. Egorova, and E. Rozanov (2008), Diurnal changes in middle atmospheric $H_2O$ and $O_3$: Observations in the Alpine region and climate models, *J. Geophys. Res.*, *113*, D17303, doi:10.1029/2008JD009892.

Hasebe, F. (1994), Quasi-biennial oscillations of ozone and diabatic circulation in the equatorial stratosphere, *J. Atmos. Sci.*, *51*, 729–745, doi:10.1175/1520-0469(1994)051<0729:QBOOOA>2.0.CO;2.

Herman, J. R. (1979), The response of stratospheric constituents to a solar eclipse, sunrise, and sunset, *J. Geophys. Res.*, *84*(C7), 3701–3710, doi:10.1029/JC084iC07p03701.

Hollandsworth, S. M., K. P. Bowman, and R. D. McPeters (1995), Observational study of the quasi-biennial oscillation in ozone, *J. Geophys. Res.*, *100*(D4), 7347–7361, doi:10.1029/95JD00193.

Huang, F. T., and C. A. Reber (2001), "Synoptic" estimates of chemically active species and other diurnally varying parameters in the stratosphere, derived from measurements from the Upper Atmosphere Research Satellite (UARS), *J. Geophys. Res.*, *106*(D2), 1655–1667, doi:10.1029/2000JD900515.

Huang, F. T., and C. A. Reber (2003), Seasonal behavior of the semidiurnal and diurnal tides, and mean flows at 95 km, based on measurements from the High Resolution Doppler Imager (HRDI) on the Upper Atmosphere Research Satellite (UARS), *J. Geophys. Res.*, *108*(D12), 4360, doi:10.1029/2002JD003189.

Huang, F. T., and C. A. Reber (2004), Nonmigrating semidiurnal and diurnal tides at 95 km based on wind measurements from the High Resolution Doppler Imager on UARS, *J. Geophys. Res.*, *109*, D10110, doi:10.1029/2003JD004442.

Huang, F. T., C. A. Reber, and J. Austin (1997), Ozone diurnal variations observed by UARS and their model simulation, *J. Geophys. Res.*, *102*(D11), 12,971–12,985, doi:10.1029/97JD00461.

Huang, F. T., H. G. Mayr, C. A. Reber, T. Killeen, J. Russell, M. Mlynczak, W. Skinner, and J. Mengel (2006a), Diurnal variations of temperature and winds inferred from TIMED and UARS measurements, *J. Geophys. Res.*, *111*, A10S04, doi:10.1029/2005JA011426.

Huang, F. T., H. G. Mayr, C. A. Reber, J. Russell, M. Mlynczak, and J. Mengel (2006b), Zonal-mean temperature variations inferred from SABER measurements on TIMED compared with UARS observations, *J. Geophys. Res.*, *111*, A10S07, doi:10.1029/2005JA011427.

Huang, F. T., H. G. Mayr, C. A. Reber, J. M. Russell, M. Mlynczak, and J. Mengel (2006c), Stratospheric and mesospheric temperature variations for the quasi-biennial and semiannual (QBO and SAO) oscillations based on measurements from SABER (TIMED) and MLS (UARS), *Ann. Geophys.*, *24*, 2131–2149, doi:10.5194/angeo-24-2131-2006.

Huang, F. T., H. G. Mayr, C. A. Reber, J. M. Russell III, M. G. Mlynczak, and J. G. Mengel (2008a), Ozone quasi-biennial oscillations (QBO), semiannual oscillations (SAO), and correlations with temperature in the mesosphere, lower thermosphere, and stratosphere, based on measurements from SABER on TIMED and MLS on UARS, *J. Geophys. Res.*, *113*, A01316, doi:10.1029/2007JA012634.

Huang, F. T., H. G. Mayr, J. M. Russell III, M. G. Mlynczak, and C. A. Reber (2008b), Ozone diurnal variations and mean profiles in the mesosphere, lower thermosphere, and stratosphere, based on measurements from SABER on TIMED, *J. Geophys. Res.*, *113*, A04307, doi:10.1029/2007JA012739.

Huang, F. T., R. D. McPeters, P. K. Bhartia, H. G. Mayr, S. M. Frith, J. M. Russell III, and M. G. Mlynczak (2010), Temperature diurnal variations (migrating tides) in the stratosphere and lower mesosphere based on measurements from SABER on TIMED, *J. Geophys. Res.*, *115*, D16121, doi:10.1029/2009JD013698.

Kaufmann, M., O. A. Gusev, K. U. Grossmann, F. J. Martin-Torres, D. R. Marsh, and A. A. Kutepov (2003), Satellite observations of daytime and nighttime ozone in the mesosphere and lower thermosphere, *J. Geophys. Res.*, *108*(D9), 4272, doi:10.1029/2002JD002800.

Lean, J. L. (1982), Observation of the diurnal variation of atmospheric ozone, *J. Geophys. Res.*, *87*(C7), 4973–4980, doi:10.1029/JC087iC07p04973.

Ling, X. D., and J. London (1986), The quasi-biennial oscillation of ozone in the tropical middle stratosphere: A one-dimensional model, *J. Atmos. Sci.*, *43*, 3122–3137, doi:10.1175/1520-0469(1986)043<3122:TQBOOO>2.0.CO;2.

Marsh, D. R., W. R. Skinner, A. R. Marshall, P. B. Hays, D. A. Ortland, and J.-H. Yee (2002), High Resolution Doppler Imager observations of ozone in the mesosphere and lower thermosphere, *J. Geophys. Res.*, *107*(D19), 4390, doi:10.1029/2001JD001505.

Pallister, R. C., and A. F. Tuck (1983), The diurnal variation of ozone in the upper stratosphere as a test of photochemical theory, *Q. J. R. Meteorol. Soc.*, *109*, 271–284, doi:10.1002/qj.49710946002.

Reber, C. A. (1993), The Upper Atmosphere Research Satellite (UARS), *Geophys. Res. Lett.*, *20*(12), 1215–1218, doi:10.1029/93GL01103.

Ricaud, P., G. Brasseur, J. Brillet, J. de La Noë, J.-P. Parisot, and M. Pirre (1994), Theoretical validation of ground-based microwave ozone observations, *Ann. Geophys.*, *12*, 664–673, doi:10.1007/s00585-994-0664-5.

Ricaud, P., J. de la Noë, B. J. Connor, L. Froidevaux, J. W. Waters, R. S. Harwood, I. A. MacKenzie, and G. E. Peckham (1996), Diurnal variability of mesospheric ozone as measured by the UARS Microwave Limb Sounder Instrument: Theoretical and ground-based validations, *J. Geophys. Res.*, *101*(D6), 10,077–10,089, doi:10.1029/95JD02841.

Rood, R. B., and A. Douglass (1985), Interpretation of ozone temperature correlations: 1. Theory, *J. Geophys. Res.*, *90*(D3), 5733–5743, doi:10.1029/JD090iD03p05733.

Rose, K., and G. Brasseur (1989), A three-dimensional model of chemically active trace species in the middle atmosphere during disturbed

winter conditions, *J. Geophys. Res.*, *94*(D13), 16,387–16,403, doi:10.1029/JD094iD13p16387.

Russell, J. M., III, M. G. Mlynczak, L. L. Gordley, J. Tansock, and R. Esplin (1999), An overview of the SABER experiment and preliminary calibration results, *Proc. SPIE Int. Soc. Opt. Eng.*, *3756*, 277–288.

Schoeberl, M. R., et al. (2006), Overview of the EOS Aura mission experiment, *IEEE Trans. Geosci. Remote Sens.*, *44*(5), 1066–1074, doi:10.1109/TGRS.2005.861950.

Tian, W., M. P. Chipperfield, L. J. Gray, and J. M. Zawodny (2006), Quasibiennial oscillation and tracer distributions in a coupled chemistry-climate model, *J. Geophys. Res.*, *111*, D20301, doi:10.1029/2005JD006871.

Vaughan, G. (1984), Mesospheric ozone—Theory and observation, *Q. J. R. Meteorol. Soc.*, *110*, 239–260.

Waters, J. W., et al. (2006), The Earth observing system microwave limb sounder (EOS MLS) on the Aura satellite, *IEEE Trans. Geosci. Remote Sens.*, *44*(5), 1075–1092, doi:10.1109/TGRS.2006.873771.

Wu, D. L., and J. H. Jiang (2005), Interannual and seasonal variations of diurnal tide, gravity wave, ozone, and water vapor as observed by MLS during 1991–1994, *Adv. Space Res.*, *35*, 1999–2004, doi:10.1016/j.asr.2004.12.018.

Zawodny, J. M., and M. P. McCormick (1991), Stratospheric Aerosol and Gas Experiment II measurements of the quasi-biennial oscillations in ozone and nitrogen dioxide, *J. Geophys. Res.*, *96*(D5), 9371–9377, doi:10.1029/91JD00517.

Zeng, Z., W. Randel, S. Sokolovsky, C. Deser, Y.-H. Kuo, M. Hagan, J. Du, and W. Ward (2008), Detection of migrating diurnal tide in the tropical upper troposphere and lower stratosphere using the Challenging Minisatellite Payload radio occultation data, *J. Geophys. Res.*, *113*, D03102, doi:10.1029/2007JD008725.

Zommerfelds, W. C., K. F. Kunzi, M. E. Summers, R. M. Bevilacqua, D. F. Strobel, M. Allen, and W. J. Sawchuck (1989), Diurnal variations of mesospheric ozone obtained by ground-based microwave radiometry, *J. Geophys. Res.*, *94*(D10), 12,819–12,832, doi:10.1029/JD094iD10p12819.

F. T. Huang, GEST, University of Maryland Baltimore County, Baltimore, MD 21228, USA. (fthuang@comcast.net)

H. G. Mayr, NASA Goddard Space Flight Center, Greenbelt, MD 20771, USA.

M. G. Mlynczak, NASA Langley Research Center, Hampton, VA 23681, USA.

J. M. Russell III, Center for Atmospheric Sciences, Hampton University, Hampton, VA 23668, USA.